St. Joseph's Journal of Humanities and Science
ISSN: 2347 - 5331
http://sjctnc.edu.in/6107-2/

MORPHOLOGY, OPTICAL, PHOTOLUMINESCENCE AND BACTERICIDAL ACTIVITY OF PRECIPITATIONAL SYNTHESIS OF CdO@ZnO CORE-SHELL PARTICLES.

- A.Vijayabalan *

Abstract

The CdO@ZnO core-shell is prepared by precipitation method and characterized by XRD, HR-SEM, DRS and photoluminesence spectra. The core-shell shows larger bactericidal activity than pristine ZnO and CdO but in the case of degradation of organic dyes both are equally effective

Keywords: UV-A light, CdO, ZnO, Rhodamine-B, E.coli.

INTRODUCTION

Core-shell nanoparticles attract much attention because they have emerged at the frontier between materials chemistry and many other fields like biomedical, pharmaceutical, optical, electronics, and catalysis; They are highly functional materials with modified properties. Sometimes properties arising from either core or shell materials can be quite different. The properties can be modified by changing the core to shell ratio itself. Because of the shell material coating, the properties of the core particle like reactivity and thermal stability can be changed.

This may modify the overall particle stability and the dispersibility of the core particle. The purpose of the coating on the core particle are many fold, such as surface modification, the ability to increase the functionality, stability, and dispersibility, controlled release of the core, reduction in consumption of precious materials, and so on. Tuning of such properties by surface modification enables the core-shell nanoparticles to be used in biomedical field, especially for bioimaging, controlled drug release, targeted drug delivery, cell labeling, and tissue engineering applications. In catalysis point of view, the main advantages of such particles are modified optical and electrical properties, chemical stability, morphology, etc. The external coating of another semiconductor material is responsible for such modifications. Reports on synthesis of core-shell nanoparticles are many [1] and Choudhuri and Paria [2] have recently listed the same. Semiconductor core-shell nanoparticles are being prepared by methods like precipitation, wet chemical reaction, precipitation in microemulsion, etc. Some of the core-shell nanoparticles prepared so far are Fe_2O_3@TiO_2 [3-7] Fe_2O_3@ZnO [8,9] CeO_2@TiO_2 [1] etc. Literature search shows that CdO@TiO_2 and CdO@ZnO core-shell nanoparticles have not been prepared so far. The conduction band of CdO core is less cathodic than those of TiO_2 and ZnO shells and the valence band hole is less anodic than those of TiO_2 and ZnO shells. ZnO–CdS core–shell hybrid nanorods as an efficient photocatalyst for hydrogen evolution from water splitting. In contrast to the previously developed ZnO–CdS heterostructures containing only ZnO/ CdS nanoparticles prepared by wet chemistry route

*Assistant Professor, Department of Chemistry, St. Joseph's College of Arts and Science (Autonomous), Cuddalore, Tamil Nadu, India. Cell: +91 9751061520, E-mail: vijayabalanchem@gmail.com

[10], ZnO–CdS core–shell nanorods show very stable hydrogen evolution in a long-term reaction under the irradiation of simulated solar light.

CHEMICALS AND EXPERIMENTS

Chemicals

Zinc nitrate (Hi-media), Cadmium Oxide (Sd-fine), Oxalic acid (Merck) and polyethylene glycol 4000 (Qualigens) were used. Commercially available ethanol was distilled over CaO. MacConkey agar (Hi-media) and nutrient broth (SRL) were used as supplied. Doubly distilled deionized water was employed throughout the experiments. Other chemicals used were also of analytical or reagent grade.

Experiments

Preparation of CdO@ZnO core-shell by precipitation method

To CdO nanoparticles suspended in distilled ethanol (0.1 g in 10 mL) under sonication for 10 min, aqueous solution of $Zn(NO_3)_2$ (5 g in 15 mL) was added drop wise with stirring. To this was added aqueous oxalic acid (0.5 M, 50 mL) to precipitates zinc oxalate. This was followed by polyethylene glycol 4000 in ethanol (10 mL, 0.01 M), also under stirring in 1 h. After thermostating for 1 h at 80 °C the solid was separated by filtration, washed, dried and calcined at 500 °C for 2 h.

RESULTS AND DISCUSSION

Structural Analysis

The X-ray diffraction pattern of CdO@ZnO core-shell particles are shown in the fig.1c. It shows the crystal structure of the ZnO shell as primitive hexagonal crystal lattice with cell parameters *a* and *b* as 0.3249 nm and *c* as 0.5205 nm. The peaks match with those of zincite (JCPDS no. 89-7102) revealing the shell as ZnO wurtzite shown in the fig.1 (b). The X-ray diffractogram of the CdO precursor used to synthesis the core-shell particles, is displayed in Fig.1 (a). The displayed XRD matches with face centered cubic lattice of CdO (JCPDS no. 65-2908), confirming the crystal structure of core CdO. The mean crystallite sizes of the precipitation synthesized CdO@ZnO, ZnO and CdO have been deduced from the half-width of the full maximum of the most intense peaks of the respective crystals using the scherrer equation, $D= 0.9\lambda /\beta \cos \theta$. Where, D is the mean crystallite size, λ is the wavelength of X-ray,θ is the bragg angle and β is the corrected half peak width of the experimental sample. The average crystal sizes of ZnO and CdO are 58 and 57 nm respectively.

Morphology

The high resolution scanning electron microscopic (HR-SEM) images of CdO@ZnO core-shell particles, at different magnifications shown in the fig.2. It is nanodimension. They are pebble like and lack definite shape. The Transmission electron microscopic (TEM) images of CdO@ZnO nanoparticles at different magnifications are shown in the fig.3.The TEM images confirm the nanoparticulate nature of the CdO@ ZnO core-shell particles.

The energy dispersive X-ray (EDX) spectra of CdO@ZnO nanoparticles are shown in fig.4 It is confirms the presence of ZnO shell in the prepared core-shell particles. They display the presence of Zn and the absence of Cd. The core CdO is deeply buried underneath the ZnO shell and the X-rays employed in the EDX analysis do not penetrate beyond the ZnO shell. It is known that X-rays penetrate only a few interplanner distances in crystals, which correspond to a few nanometers of the ZnO shell. The EDX spectrum of crushed CdO@ZnO particles is presented in the fig.5.The core-shell particles were grounded well in an agate pestle and mortar. The EDX spectrum shows the presence of Cd in addition to Zn. This is due to the broken ZnO shell; crushing breaks the shell of some core-shell particles and exposes the CdO core to X-ray in EDX analysis.

The selected area electron diffraction (SAED) pattern of CdO@ZnO are shown in the fig.6.It is confirms the presence of CdO core in CdO@ZnO core-shell particles. The interplanar distances corresponding to the displayed concentric diffraction rings match with those of primitive hexagonal ZnO lattice shell and face centered cubic CdO lattice core; the JCPDS patterns used for indexing are 89-7102 and 65-2908 respectively.

Optical Property

The diffuse reflectance spectra (DRS) of CdO@ ZnO core-shell particles are shown in fig7. The DRS are presented in terms of $F(R)$, obtained by the application of Kubelka-Munk algorithm $F(R) = (1 - R^2)/2R$, where R is the reflectance. The DRS of core-shell particles show that they absorb UV-A light but not visible light. This confirms the ZnO shell in the prepared core-shell particles. Also, it infers that the synthesized materials are not CdO-ZnO composites; CdO absorbs visible light. The direct band gaps of CdO@ZnO particles, have been deduced from Tauc plots of $[F(R)hv]^2$ *versus* hv, as displayed in fig.8.The Tauc plots of $[F(R)hv]^{0.5}$ *versus* photon energy, which give the indirect band gaps of the core-shell oxides shown in fig.9. The deduced band gaps of CdO@ZnO are comparable with that of ZnO but not with that of precursor CdO. This confirms the perfect ZnO shell of the synthesized core-shell particles. The direct and indirect band gaps of CdO are deduced through Tauc plots as shown in figs. 8 and 9. respectively.

Photoluminescence

The photoluminescence (PL) spectra of CdO@ZnO core-shell particles are presented in fig.10. The PL spectra of ZnO adopting the procedure followed for the synthesis of core-shell oxides but without using CdO. The emission spectrum of CdO@ZnO is similar to that of bare ZnO. The CdO@ZnO and ZnO show near band gap emission (NBE) at 424 nm. This is due to excitonic recombination [11].These emissions are close to the band gap absorptions, shown by the Kubelka-Munk plots. Further, they show blue or deep level emission (DLE) at 458 nm. The visible emission is due to the recombination of electron in singly occupied oxygen vacancy with the photogenerated hole in the VB. The DLE is related to structural defects and strong DLE indicates more defects [12].

Photodegrdation Process

The photocatalytic activities of CdO@ZnO particles have been examined under UV-A light using rhodamine B as test substrate are shown in the fig.11. The results are corrected for adsorption. The profiles of dye degradation on pristine ZnO and CdO precursor are also presented in Fig.11. for comparison. The photocatalytic activity of CdO@ZnO and ZnO both are same. As expected CdO, shows poor photocatalytic activity. Generally CdO is a less efficient photocatalyst [13]. Photoformation of electron-hole pairs, their recombination, interfacial charge transfer, light absorption efficiency, adsorption of water molecule, molecular oxygen and dye molecule, etc., determines the photocatalytic efficiency of a semiconductor. ZnO is a better photocatalyst than CdO. The conduction band (CB) electron in ZnO is more cathodic than that of CdO and also the valence band (VB) hole of ZnO is more anodic than that of CdO. This is expected to decrease the photocatalytic activity. That is, the core-shell oxides are to be less photocatalytically active than pristine ZnO. The photoexcited electron in the CB of ZnO in CdO@ZnO is expected to move to the CB of CdO. Similarly, the photogenerated hole in the VB of ZnO in CdO@ZnO is expected to slip to the VB of CdO [14].The energy positions of the CB edges and VB edges of ZnO and CdO on the absolute vacuum scale (AVS) is presented in Fig.12 [14]. They determine the charge transfer from ZnO to CdO. The energy difference between the CB electrons of ZnO and CdO is the driving force for the interparticle electron injection and the free energy change is given by $-\Delta G = e[E_{CB(CdO)} - E_{CB(ZnO)}]$[15]. Similarly, the energy difference between the VB holes of ZnO and CdO is responsible for the interparticle hole injection. This movement of photogenerated electron and hole from ZnO shell to CdO core should result in recombination of the photogenerated charge carriers in CdO core thus suppressing the photocatalytic activity. This is observed in hydrothermally synthesized CdO@ZnO.

Antibacterial Activity

The time profiles of *E. coli* disinfection by CdO@ ZnO shown in the figs.13. The displayed disinfections are by the core-shell particles in aqueous suspension in absence of direct illumination. The corresponding profile of *E. coli* inactivation by pristine ZnO and CdO are also shown in Fig.13. for comparison. In absence of the particles the *E. coli* population remains unaffected during the experimental period displaying the bactericidal activity of the particles tested. *E. coli* bacteria in 0.9% saline were used for the evaluation of the bactericidal activity. The cell population was determined by a viable count method on MacConkey

agar plates after proper dilution of the culture. The temporal profiles show larger bactericidal activity of CdO@ZnO than pristine CdO and ZnO.

CONCLUSION

The prepared CdO@ZnO core-shell was confirmed by XRD and EDX. The photocatalytic degradation of rhodamine B suppressed and *E.coli* enhanced by core-shell in UV and dark respectively. The deep level emission is strong for CdO@ZnO core-shell is due to crystal defects.

REFERENCES

1. D.N. Correa, J.M. De se Silva, E.B. Santos, F.A. Sigoli, A.G.S. Filho and I.O. Mazali, *J. Phys. Chem. C,* **2011**, *115*, 10380.
2. R.G. Choudhuri and S. Paria, *Chem. Rev.,* **2012***, 112,* 2373.
3. R. Amal, G. Low and S. McEvoy, ***J. Phys. Chem. B***, **2000**, *104***,** 4387.
4. Y. Ao, J. Xu, D. Fu, X. Shen and C. Yuan, *Sep. Purif. Technol.* **2008**, *61*,436.
5. S. H. Xuan, W. Q. Jiang, X. L. Gong, Y. Hu and Z. Y. Chen, ***J. Phys. Chem. C*****, 2009**, *113*, *553***.**
6. X. Xu and V. Cabuil, ***J. Nanopart. Res***., **2009**, *11*, 459**.**
7. M. Kang, S. J. Choung and J.Y. Park, *Catal. Today,* **2003**, *87*, 87.
8. J. Wan, H. Li and K. Chen, *Mater. Chem. Phys.,* **2009***, 114*, 30.
9. W. Yan, H. Fan and C. Yang*, Mater. Lett.,* **2011**,*65*,1595.
10. Jing DW, Guo LJ. A novel method for the preparation of a highly stable and active CdS photocatalyst with a special surface nanostructure. J Phys Chem B **2006**; 110(23):11139–45.
11. T.Sun, J.Qiu and C.Liang, *J.Phys. Chem.C,* **2008**,*112*,715.
12. M-K.Lee, T.G.Kim, W.Kim and Y-M,Sung, *J.Phys. Chem.C*, **2008,** *112,* 10079.
13. C.Karunakaran, S.Senthilvelan, S.Karuthapandian and K.Balaraman, *Catal.Commun*.**2004**, *5*, 283
14. Y.Xu and M.A.A Schoren, *Am.Mineral*, **2000,** *85*, 543.
15. R.Katosh, A.Furube, T.Yoshihara, K.Hara, G.Fujihashi, S.Takano, S.Murata, H.Arakawa and M.Tachiya, *J.Phys.Chem.B*; **2004,** *108*, 4818.

Graphical Abstract

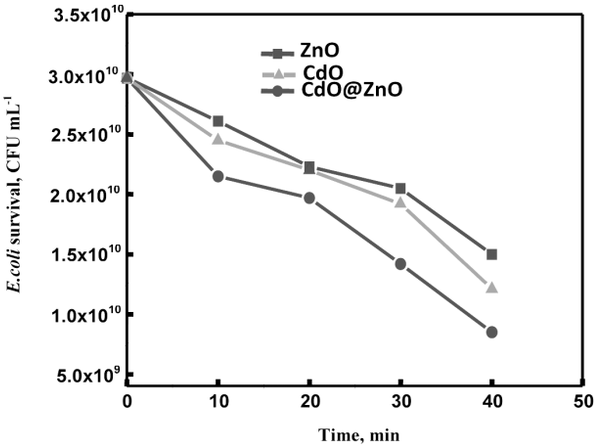

- The prepared CdO@ZnO core-shell is more efficient inactivation of bacteria than ZnO and CdO under dark.
- The prepared core-shell is nanodimension.
- Core-shell was used for mineralization process.

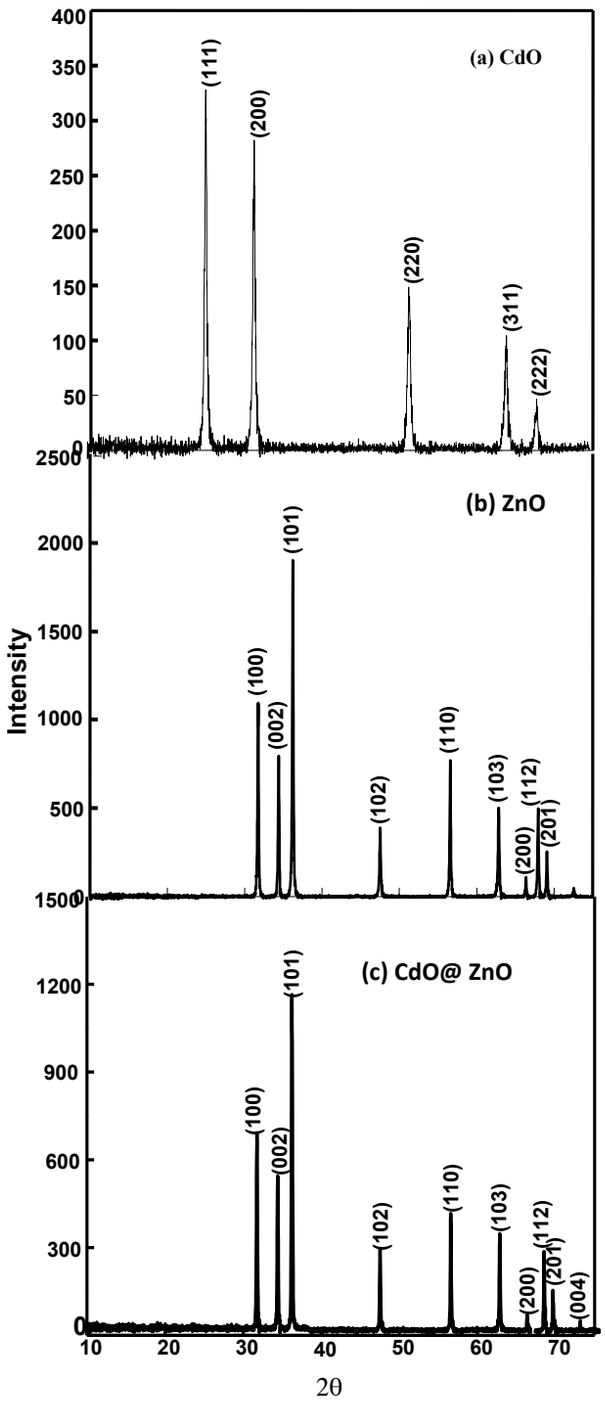

Fig.1: XRD spectra of CdO, ZnO and core-shell

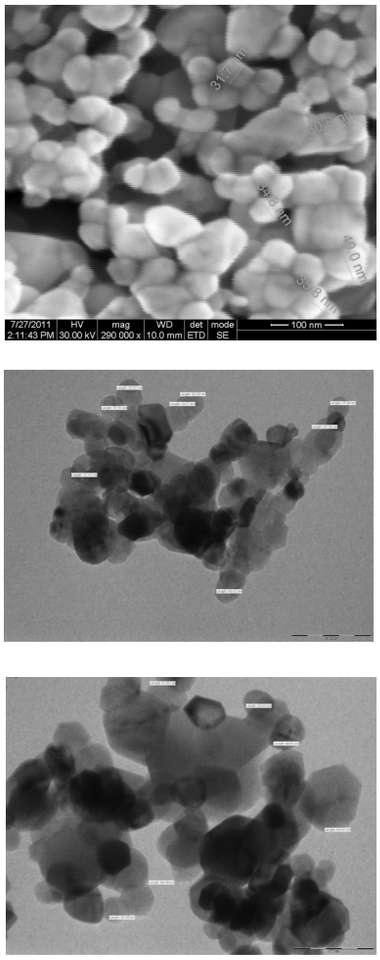

Fig.2 : HR-SEM images of precipitation synthesis of CdO@ZnO core-shell

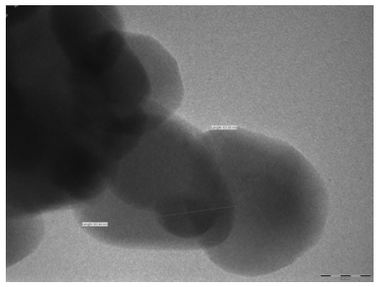

Fig.3 : TEM images of precipitation synthesis of CdO@ZnO core-shell

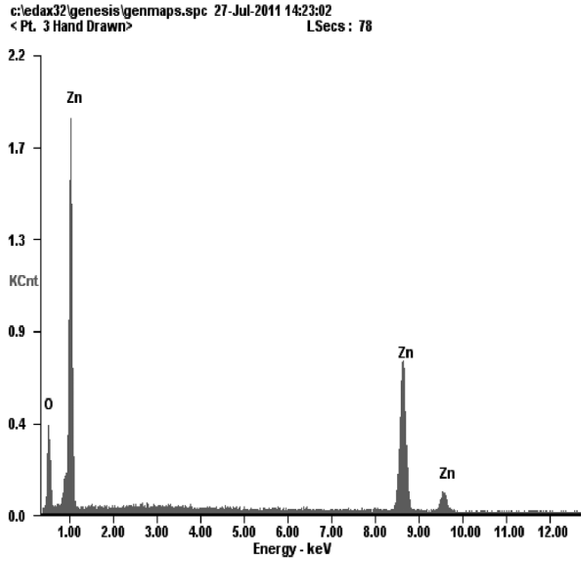

Fig.4 : EDX spectrum of CdO@ZnO core-shell

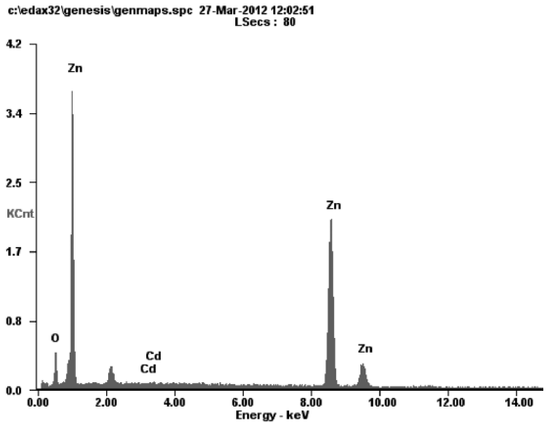

Fig.5 : EDX spectrum of crushed CdO@ZnO core-shell

Element	Wt%	At%
OK	14.05	40.11
CdL	00.62	00.25
ZnK	85.33	59.63
Total	100	100

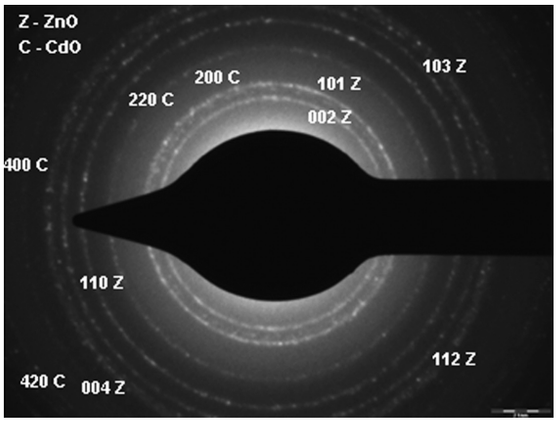

Fig. 6 : The SAED pattern of precipitation synthesized CdO@ZnO core-shell

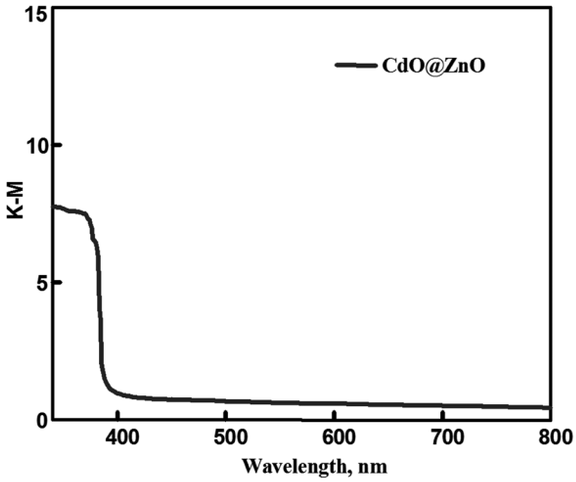

Fig.7 : DRS spectrum of CdO@ZnO core-shell

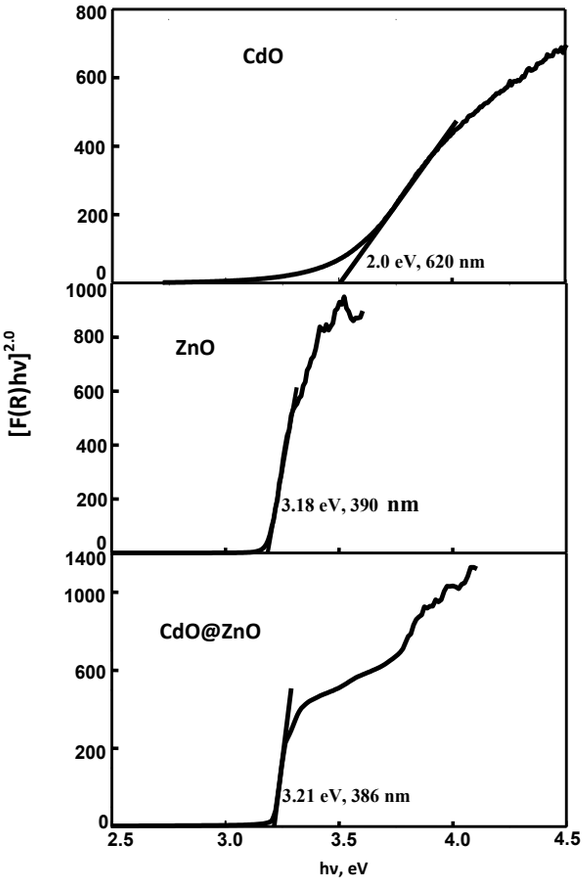

Fig.8 : Tauc plot for direct bandgap

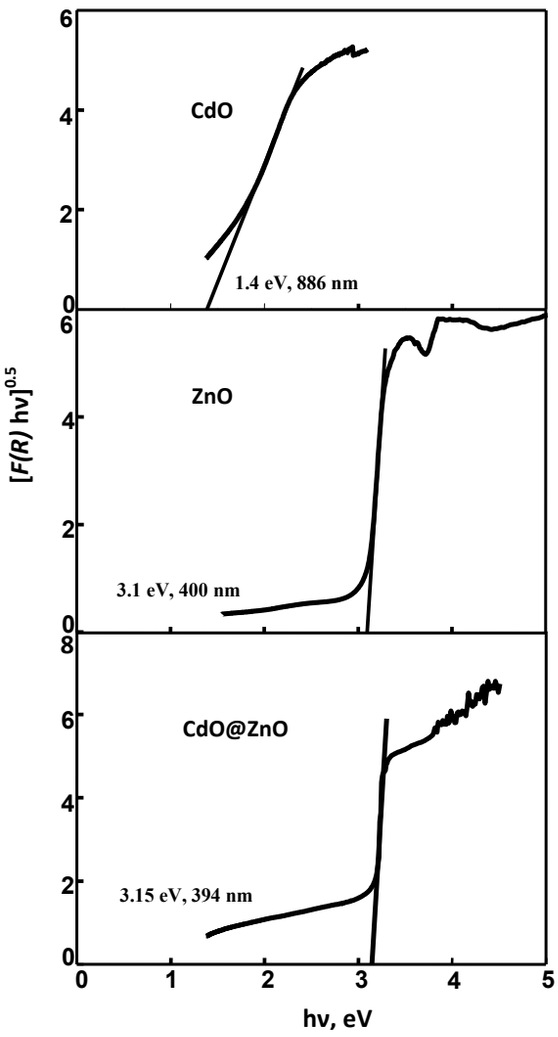

Fig.9 : Tauc plot for indirect bandgap

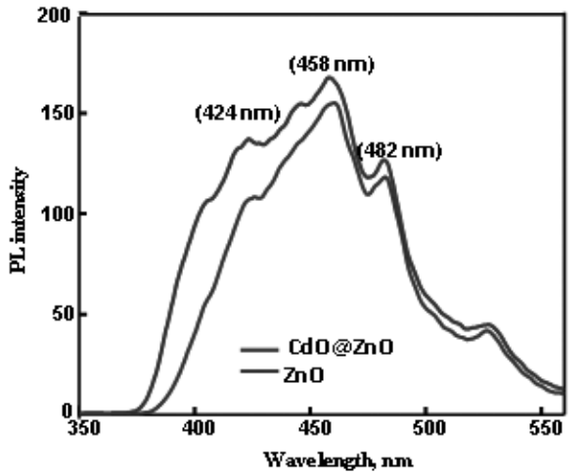

Fig.10 : Photoluminescence spectra

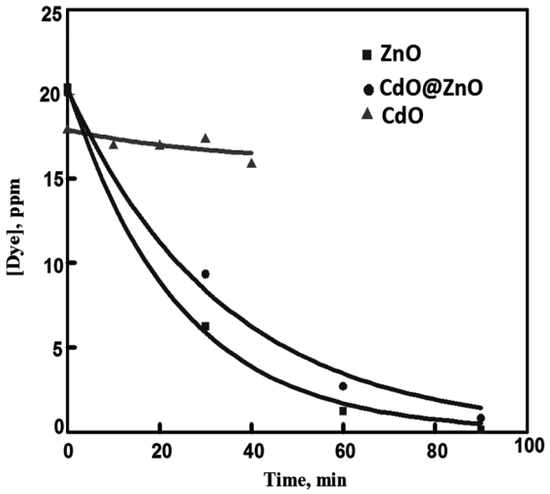

Fig.11 : Time profile for dye degradation

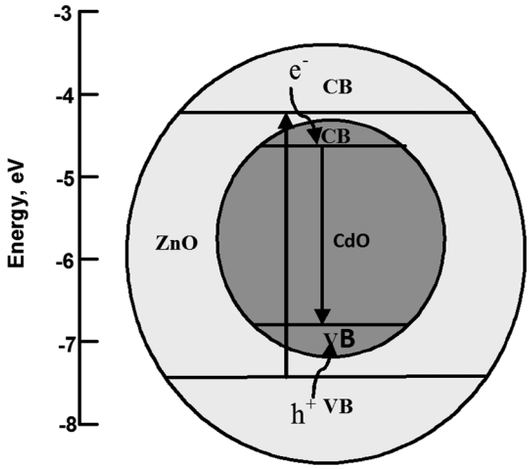

Fig.12 : Band gap energy level (AVS) of CdO@ ZnO

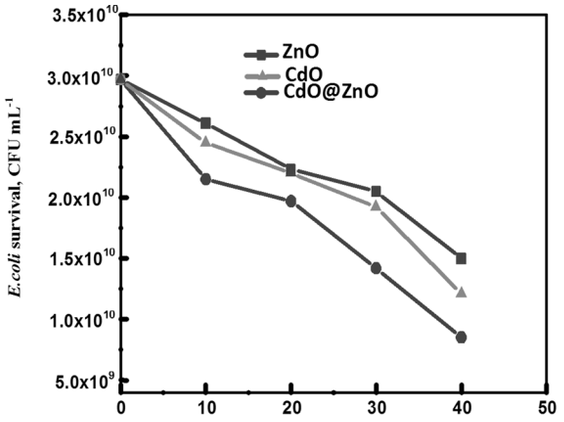

Fig.13 : Time profiles for disinfection of bacteria